Diagn Interv Radiol 2020; 26:557–564
© Turkish Society of Radiology 2020

CHEST IMAGING
ORIGINAL ARTICLE

Visual and software-based quantitative chest CT assessment of COVID-19: correlation with clinical findings

Gamze Durhan
Selin Ardalı Düzgün
Figen Başaran Demirkazık
İlim Irmak
İlkay İdilman
Meltem Gülsün Akpınar
Erhan Akpınar
Serpil Öcal
Gülçin Telli
Arzu Topeli
Orhan Macit Arıyürek

PURPOSE
The aim of this study was to evaluate visual and software-based quantitative assessment of parenchymal changes and normal lung parenchyma in patients with coronavirus disease 2019 (COVID-19) pneumonia. The secondary aim of the study was to compare the radiologic findings with clinical and laboratory data.

METHODS
Patients with COVID-19 who underwent chest computed tomography (CT) between March 11, 2020 and April 15, 2020 were retrospectively evaluated. Clinical and laboratory findings of patients with abnormal findings on chest CT and PCR-evidence of COVID-19 infection were recorded. Visual quantitative assessment score (VQAS) was performed according to the extent of lung opacities. Software-based quantitative assessment of the normal lung parenchyma percentage (SQNLP) was automatically quantified by a deep learning software. The presence of consolidation and crazy paving pattern (CPP) was also recorded. Statistical analyses were performed to evaluate the correlation between quantitative radiologic assessments, and clinical and laboratory findings, as well as to determine the predictive utility of radiologic findings for estimating severe pneumonia and admission to intensive care unit (ICU).

RESULTS
A total of 90 patients were enrolled. Both VQAS and SQNLP were significantly correlated with multiple clinical parameters. While VQAS >8.5 (sensitivity, 84.2%; specificity, 80.3%) and SQNLP <82.45% (sensitivity, 83.1%; specificity, 84.2%) were related to severe pneumonia, VQAS >9.5 (sensitivity, 93.3%; specificity, 86.5%) and SQNLP <81.1% (sensitivity, 86.5%; specificity, 86.7%) were predictive of ICU admission. Both consolidation and CPP were more commonly seen in patients with severe pneumonia than patients with nonsevere pneumonia ($P = 0.197$ for consolidation; $P < 0.001$ for CPP). Moreover, the presence of CPP showed high specificity (97.2%) for severe pneumonia.

CONCLUSION
Both SQNLP and VQAS were significantly related to the clinical findings, highlighting their clinical utility in predicting severe pneumonia, ICU admission, length of hospital stay, and management of the disease. On the other hand, presence of CPP has high specificity for severe COVID-19 pneumonia.

From the Departments of Radiology (G.D. ✉ *gamzedurhan@gmail.com*, S.A.D., F.B.D., İ.İ., M.G.A., E.A., O.M.A.), Pulmonary Medicine (İ.I.), Intensive Care, Department of Internal Medicine, Division of Intensive Care (S.Ö., A.T.), and Infectious Diseases (G.T.), Hacettepe University School of Medicine, Ankara, Turkey.

Received 28 May 2020; revision requested 22 June 2020; last revision received 20 July 2020; accepted 4 August 2020.

Published online 31 August 2020.

DOI 10.5152/dir.2020.20407

A novel type of betacoronavirus (severe acute respiratory syndrome coronavirus 2, SARS-CoV-2) has been identified since December 2019 among patients with pneumonia presenting with fever, cough, dyspnea, myalgia, and fatigue (1, 2). The disease caused by this virus was officially named as coronavirus disease 2019 (COVID-19) by the World Health Organization (WHO).

The clinical spectrum of COVID-19 is variable and includes asymptomatic infections, mild respiratory disease, severe pneumonia and acute respiratory distress syndrome (ARDS) (3). Lungs are the main area of involvement in COVID-19, and the possible underlying pathologic mechanism was reported as inflammatory exudation and diffuse alveolar damage (4). Although COVID-19 is typically confirmed by real-time reverse-transcription polymerase chain reaction (RT-PCR) from swab samples, the low sensitivity (60%–70%) of the test is a major issue in the clinical setting (5, 6). In this regard, chest CT has emerged as an ancillary

You may cite this article as: Durhan G, Ardalı Düzgün S, Başaran Demirkazık F, et al. Visual and software-based quantitative chest CT assessment of COVID-19: correlation with clinical findings. Diagn Interv Radiol 2020; 26:557–564

clinical tool, which plays a key role in both diagnosis and management of the disease. Common CT findings of COVID-19 have been defined as bilateral patchy ground glass opacities (GGOs) with peripheral predominance in recent studies (7). Besides diagnosis, quantitative CT evaluation can give information about the clinical severity of the disease and prognosis. Quantitative analysis can be performed visually or by the use of software-based algorithms (8–10). While visual quantitative assessment score (VQAS) has an inherent subjectivity, software-based quantitative assessment of the normal lung parenchyma percentage (SQNLP) has some challenges such as quality of training data, inaccurate preprocessing steps, artifacts due to patient or respiratory motion. Despite these challenges, SQNLP has a growing role in diagnosis, determination of prognosis and longitudinal management of patients with diffuse lung diseases (11). As COVID-19 can cause diffuse lung disease, quantitative evaluation of abnormal regions and normal parenchyma on chest CT might have a clinical utility from the perspective of management decisions and prognostic predictions.

In this study, we evaluated the normal lung parenchyma with SQNLP, lung opacities with VQAS, noted the presence of consolidation and crazy paving pattern (CPP) in COVID-19 pneumonia, and determined the relationship of these radiologic findings with each other, as well as with the clinical and laboratory data of the patients.

Methods

Approval for the study was granted by the local ethics committee (approval number: 2020/08-04, project number: GO 20/390). Informed consent was not required because of the retrospective nature of the study.

Main points

- Both SQNLP and VQAS were significantly related to the clinical findings, highlighting their clinical utility in predicting severe pneumonia, ICU admission, length of hospital stay, and management of the disease.
- While VQAS >8.5 and SQNLP <82.45% can show severe pneumonia, VQAS >9.5 and SQNLP <81.1% can predict ICU admission with high sensitivity and specificity.
- Crazy paving pattern has high specificity (97.2%) for severe COVID-19 pneumonia.

Patients

A retrospective review was made of 588 consecutive adult patients (>18 years old) who underwent chest CT for investigating COVID-19 pneumonia between March 11, 2020 and April 15, 2020. Exclusion criteria were: 1) negative RT-PCR assay for SARS-CoV-2; 2) negative chest CT; 3) coinfection by other pathogens; 4) inappropriate CT images including respiratory artifacts or CT images taken in expiratory phase; 5) inadequate segmentation by the software. Study flowchart is presented in Fig. 1. Finally, a total of 90 patients were included in the study.

All clinical data and laboratory data of patients are shown in detail in Tables 1 and 2. A clinical model of National Health Commission was used (12). According to this model, patients were divided into two groups as severe and nonsevere pneumonia of COVID-19. Severe pneumonia was defined as having typical symptoms (e.g., fever, sore throat, cough, myalgia) and respiratory rate ≥30 breaths/min, resting oxygen saturation <90% and at least one of the poor prognostic factors in blood tests at admission such as lymphocyte count $<0.8\times10^9$ /L, C-reactive protein (CRP) >4 mg/dL, ferritin >500 µg/L or d-dimer >1 µg/L.

CT protocol

The patients were examined in a supine position with arms raised and instructed to hold their breath during acquisition. Unenhanced chest CT scans were acquired from the apex to the lung bases. CT scans were acquired on third generation dual source CT scanner (Somatom Force, Siemens Healthineers). Online dose modulation (Care DOSE 4D, Siemens Medical Solutions)

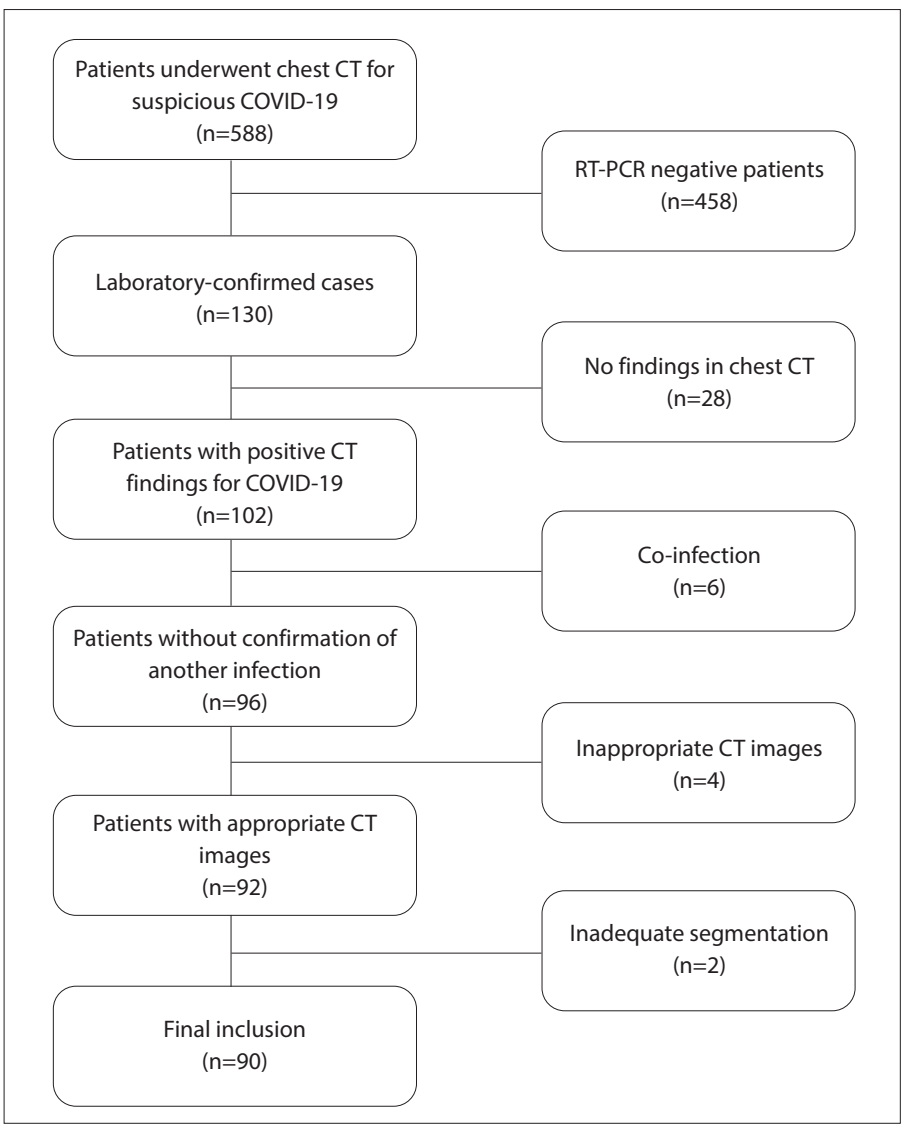

Figure 1. Flowchart shows patients excluded from the study and the reasons for exclusion.

Table 1. Clinical characteristics and radiological scores of patients

	Total (n=90)	Severe (n=19)	Non-severe (n=71)	*P*
Age (years)	45.0±14.4	54.6±12.9	42.4±13.8	0.001
Sex (female/male)	43/47	3/16	40/31	0.002
Smoking history, n (%)				
Unknown	10 (11.1)	3 (15.8)	7 (9.9)	0.435
Never	62 (68.9)	11 (57.9)	51 (71.8)	0.244
Former	10 (11.1)	4 (21.0)	6 (8.4)	0.209
Current	8 (8.9)	1 (5.3)	7 (9.9)	1
Comorbidities, n (%)	31 (34.4)	12 (63.1)	19 (26.7)	0.003
Hypertension	15 (16.6)	5 (26.3)	10 (14)	0.295
Diabetes mellitus	6 (6.6)	2 (10.5)	4 (5.6)	0.603
Immunosupression	5 (5.5)	4 (21)	1 (1.4)	0.007
Cardiovascular disease	4 (4.4)	1 (5.2)	3 (4.2)	1
Asthma	4 (4.4)	1 (5.2)	3 (4.2)	1
Malignancy	3 (3.3)	1 (5.2)	2 (2.8)	0.513
Autoimmune diseases	3 (3.3)	2 (10.5)	1 (1.4)	0.112
Chronic kidney disease	1 (1.1)	1 (5.2)	0 (0)	0.211
Chronic liver disease	1 (1.1)	1 (5.2)	0 (0)	0.211
COPD	1 (1.1)	0 (0)	1 (1.4)	1
Symptoms, n (%)				
Fever	50 (55.5)	11 (57.8)	39 (54.9)	0.817
Dry cough	63 (70)	12 (63.1)	51 (71.8)	0.464
Weakness	47 (52.2)	11 (57.8)	36 (50.7)	0.577
Myalgia	43 (47.7)	7 (36.8)	36 (50.7)	0.283
Sore throat	24 (26.6)	4 (21)	20 (28.1)	0.533
Headache	15 (16.6)	2 (10.5)	13 (18.3)	0.729
Dyspnea	17 (18.8)	9 (47.3)	8 (11.2)	<0.001
Anosmia	12 (13.3)	1 (5.2)	11 (15.4)	0.448
Diarrhea	10 (11.1)	2 (10.5)	8 (11.2)	1
Nasal congestion and runny nose	8 (8.8)	0 (0)	8 (11.2)	0.195
Chest pain	8 (8.8)	1 (5.2)	7 (9.8)	1
Expectoration	5 (5.5)	0 (0)	5 (7)	0.580
Conjunctivitis	2 (2.2)	1 (5.2)	1 (1.4)	0.380
Hemoptysis	1 (1.1)	1 (5.2)	0 (0)	0.211
Fever at admission, n (%)				
37.3–38 °C	28 (31.1)	5 (26.3)	23 (32.3)	0.611
38.1–39 °C	20 (22.2)	7 (36.8)	13 (18.3)	0.119
>39 °C	2 (2.2)	0 (0)	2 (2.8)	1
Fever during follow-up, n (%)	34 (37.7)	14 (73.6)	20 (28.1)	<0.001
Oxygen therapy, n (%)	19 (21.1)	19 (100)	0 (0)	
Respiratory rate at admission	20±3	25±5	18±2.0	<0.001
Duration from symptom onset to admission (days)	5±3.1	6±3.9	5±2.9	0.226
Length of hospital stay (days)	7.1±7	16.1±11	4.7±3.1	<0.001
ICU admission, n (%)	15 (16.6)	14 (73)	1 (1.4)	
VQAS	6.7±4.0	12.4±3.7	5.1±3.7	<0.001
SQNLP	82.9±11.5	69.0±14.9	86.6±6.6	<0.001
Consolidation, n (%)	45 (50)	12 (63.2)	33 (46.4)	0.197
CPP, n (%)	11 (12.2)	9 (47.3)	2 (2.8)	<0.001

Data are presented as mean ± standard deviation or n (%).
COPD, chronic obstructive pulmonary disease, ICU, intensive care unit; VQAS, visual quantitative assessment score; SQNLP, software-based quantitative assessment of the normal lung parenchyma percentage; CPP, crazy paving pattern.

was used. Scanning parameters were as follows: tube current 50–120 mAs, tube voltage 70-120 kV, pitch 3, matrix 512×512, field of view 350×350 mm and slice thickness 3 mm. Reconstruction was performed with slice thickness of 1 mm. The CT images of patients who could not hold their breath in the inspiratory phase were excluded from the study, as, texture analysis of the images in inspiratory phase can be different from that in the expiratory phase.

Evaluation of CT images

VQAS was performed according to the extent of opacities (including GGOs, CPP and consolidation) in each lobe. Scores were defined as following: 0 (none), 1 (affecting <5% of the lobe), 2 (affecting 5%–25% of the lobe), 3 (affecting 26%–49% of the lobe), 4 (affecting 50%–75% of the lobe) and 5 (affecting >75% of the lobe). So, a maximum CT score of 5 was possible for each lobe. Total CT score was reached by summing the scores in five lobes (range from 0 to 25) (13). Previous studies have demonstrated that CT findings such as GGO, CPP (GGO with superimposed interlobular and intralobular septal thickening) (Fig. 2) and consolidation are associated with progression of COVID-19 pneumonia (13, 14). So, presence of CPP and consolidation was also noted for each patient separately. All CT images were evaluated by two radiologists (G.D. and F.D.) blinded to clinical data, with 13 and 25 years of experience, respectively. Final CT scores were determined by consensus.

SQNLP of the normal lung parenchyma was performed on the workstation by using a dedicated software (3D Pulmo, Syngovia, Siemens Healthineers). After automatic lung segmentation, analysis of normal lung parenchyma was obtained according to the attenuation values between -750 HU and -950 HU (15). If the lung segmentation was deemed to be inappropriate, lung contours were drawn manually by a radiologist (S.A.D., with 8 years of experience) who was blinded to the clinical and VQAS data. Percentage of SQNLP was noted for all patients (Figs. 3, 4).

Statistical analysis

Data obtained in the study were analyzed statistically using IBM SPSS Statistics 23.0 software. Normality of the variables was tested by Kolmogorov-Smirnov test. Descriptive statistics of the categorical data were presented as n (%); non-normalized variables were shown as median (interquar-

Table 2. Laboratory findings of patients

	Normal range*	Total (n=90)	Severe (n=19)	Non-severe (n=71)	*P*
WCC (×10⁹/L)	4.1–11.2	4.8 [2.0]	5.4 [2.0]	4.8 [2.0]	0.308
Neutrophil count (×10⁹/L)	1.8–6.4	3.1 [1.9]	3.5 [2.9]	2.9 [1.7]	0.035
Lymphocyte count (×10⁹/L)	1.2–3.6	1.1 [0.5]	0.9 [0.6]	1.1 [0.6]	0.010
NLR		2.6 [2.3]	3.7 [3.7]	2.45 [1.1]	0.004
Platelet count (×10⁹/L)	159–388	172±48	174±63.9	177±43	0.029
Hemoglobin (g/dL)	11.7–15.5	14 [2]	14.2 [2.7]	13.5 [1.8]	0.916
Ferritin (µg/L)	11–307	124 [269]	613.4 [1281]	77.5 [140]	<0.001
CRP (mg/dL)	0–0.8	1.1 [1.7]	6.9 [11.9]	0.48 [1.2]	<0.001
Procalcitonin (ng/mL)	0–0.1	0.03 [0.04]	0.08 [0.09]	0.03 [0.02]	<0.001
AST (U/L)	<35	29 [13]	39 [37]	26 [10]	0.010
ALT (U/L)	<35	25 [29)	29 [36]	21 [25]	0.395
Total bilirubin (mg/dL)	0.3–1.2	0.5 [0.3]	0.68 [0.4]	0.52 [0.2]	0.153
Albumin (g/dL)	3.5–5.2	4.1 [0.4]	3.9 [0.6]	4.2 [0.3]	<0.001
LDH (U/L)	<247	210 [89]	278 [231]	180 [79]	<0.001
D-dimer (µg/L)	0–0.55	0.3 [0.5]	0.86 [2]	0.32 [0.1]	<0.001
Fibrinogen (mg/dL)	180–350	393±127	455±182	361±85	<0.001
CK (U/L)	<145	106 [137]	131 [209]	83 [91]	0.097
BUN (mg/dL)	620	13.1 [6.1]	14.1 [9.6]	11.8 [4]	0.007
Creatinine (mg/dL)	0.51–0.95	0.7 [0.3]	0.8 [0.4]	0.7 [0.3]	0.005
Sodium (mEq/L)	136–146	138 [3]	136 [2]	138 [2]	<0.001
Potassium (mEq/L)	3.5–5.1	4 [0.5]	3.9 [0.5]	4 [0.4]	0.159
Troponin (ng/L)	8.4–18.3	3.6 [3.3]	5.4 [4.4]	3.1 [1.1]	<0.001

Continuous variables of normal distribution are expressed as mean ± SD, continuous variables of skewed distribution are shown as median [interquartile range, IQR].
WCC, white cell count; NLR, neutrophil-to-lymphocyte ratio; CRP, C-reactive protein; AST, aspartate aminotransferase; ALT, alanine transaminase; LDH, lactate dehydrogenase; CK, creatine kinase, BUN, blood urea nitrogen.
*Normal range shows reference ranges for blood tests in healthy adults.

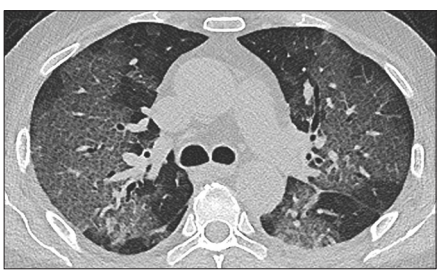

Figure 2. A 55-year-old male patient with COVID-19 pneumonia. CT image shows crazy paving pattern in both lungs.

tile range, IQR) and normal distributions were shown as mean ± standard deviation. Categorical variables were compared using the Pearson chi-square or Fisher's exact test and continuous variables were compared using the Student's t test or Mann-Whitney U test. The degree of association between continuous and/or ordinal variables was calculated by using the Pearson's correlation coefficient or Spearman's correlation coefficient. The receiver operating characteristic (ROC) curve was used to describe the diagnostic performance of the VQAS and SQNLP for determining severe pneumonia and ICU admission. The area under the ROC curve (AUC) and 95% confidence interval (95% CI) were calculated. Cutoff ranges were calculated around the optimal cutoff to maximize sensitivity and specificity to differentiate severe pneumonia and ICU admission by using the Youden index. For all tests, a two-tailed *P* value of <0.05 was considered statistically significant.

Results

Patient characteristics, clinical and laboratory findings are shown in detail in Tables 1 and 2. Only one patient with severe pneumonia died in this cohort; all other patients were discharged. Although the number of males and females was similar in total, COVID-19 pneumonia was more severe in men than in women ($P = 0.002$). Also, patients with severe pneumonia were older, had more comorbidities, and were more likely to present with dyspnea and higher fever. Most of the laboratory findings of patients with severe pneumonia were significantly different from the patients with non-severe pneumonia (Table 2).

According to CT findings, lower lobes were affected more commonly than upper lobes ($P < 0.001$) (Fig. 5). While 50% of patients had consolidation, 12.2% of patients had CPP.

There was a good degree of inverse correlation between VQAS and SQNLP (r= -0. 77, $P < 0.001$) (Fig. 6). Patients with consolidation showed higher VQAS and lower SQNLP values than patients without consolidation (for VQAS $P = 0.006$; for SQNLP $P < 0.001$). Patients with CPP had higher VQAS and lower SQNLP than patients without CPP ($P < 0.001$ for both VQAS and SQNLP).

Both VQAS and SQNLP were significantly correlated with multiple clinical and labo-

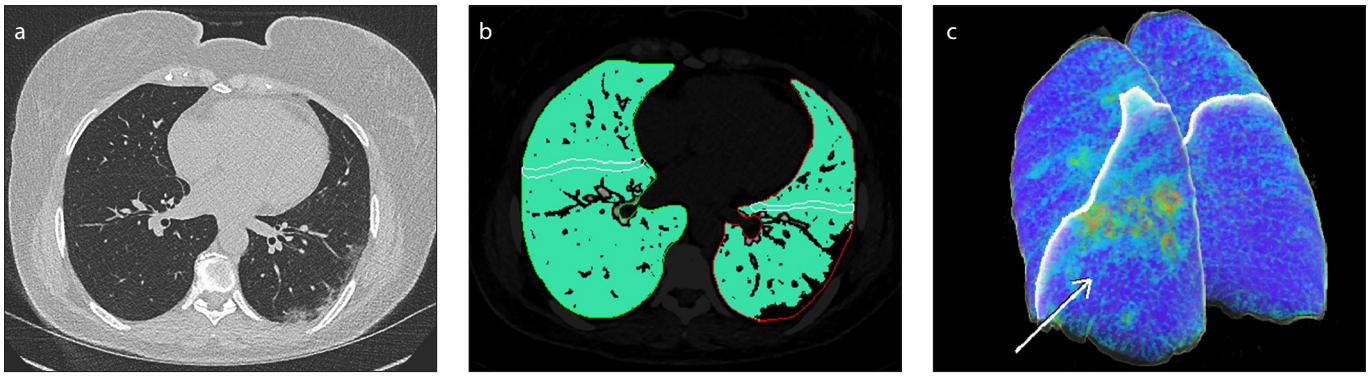

Figure 3. a–c. A 48-year-old female patient with COVID-19 pneumonia. Transverse CT scan **(a)** shows ground glass opacities in left lower lobe of the lung. Image **(b)** shows software-based automatic quantification *(green)* of normal aerated parenchyma at the threshold of -750/-950 HU. Volume rendering image **(c)** of the same patient demonstrates the involvement of the lung *(white arrow)* according to the density of lung.

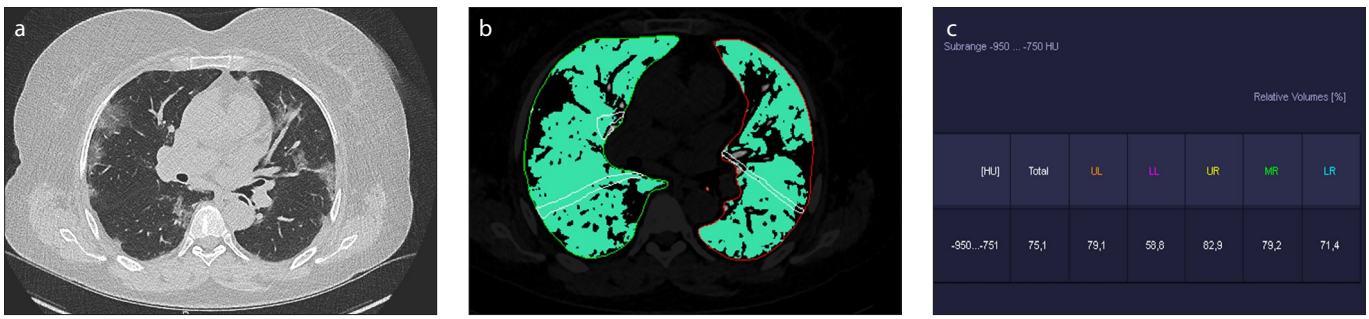

Figure 4. a–c. A 51-year-old female patient with COVID-19 pneumonia. Transverse CT scan **(a)** demonstrates bilateral patchy ground glass opacities with peripheral predominance. Software-based quantification of normal aerated parenchyma is shown in green color **(b)**. Percentage of quantification of normal parenchyma is shown for each lobe and total lung **(c)**.

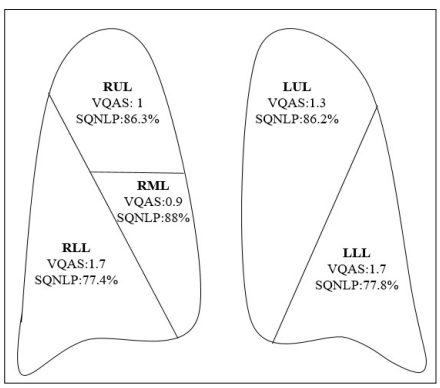

Figure 5. Involvement of lung lobes are shown according to the mean values of visual quantitative assessment score (VQAS) and software-based quantitative assessment of the normal lung parenchyma percentage (SQNLP) in patients with COVID-19 pneumonia. Lower lobes were influenced more than upper lobes ($P < 0.001$). RUL, right upper lobe; RML, right middle lobe; RLL, right lower lobe; LUL, left upper lobe; LLL, left lower lobe.

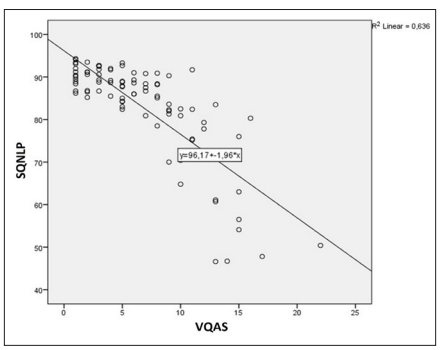

Figure 6. SQNLP and VQAS is shown with scatter plot diagram.

ratory findings including length of hospital stay, high fever, respiratory rate, old age, troponin, D-dimer, ferritin, lactate dehydrogenase (LDH), CRP, fibrinogen, sodium, albumin, and procalcitonin (Table 3).

Higher VQAS and lower SQNLP were shown in male patients and patients with dyspnea, severe pneumonia and ICU admission. On the other hand, patients with anosmia showed lower VQAS and higher SQNLP (Table 3).

The other clinical, laboratory findings and patient characteristics including smoking history, duration from symptom onset to admission, dry cough, weakness, myalgia, sore throat, headache, expectoration, hemoptysis, chest pain, diarrhea, nasal congestion, fever during follow-up, aspartate aminotransferase, alanine aminotransferase, creatinine, potassium, neutrophil-to-lymphocyte ratio (NLR), creatine kinase, bilirubin, blood urea nitrogen, hemoglobin, white blood count, neutrophil count, lymphocyte count and platelet count (Tables 1 and 2) were not significantly correlated with radiologic findings ($P > 0.05$). For identifying severe pneumonia, the optimal cutoff value was 8.5 for VQAS (sensitivity, 84.2%; specificity, 80.3%; AUC, 0.916; 95% CI, 0.852–0.980, $P < 0.001$) and 82.45% for SQNLP (sensitivity, 83.1%; specificity, 84.2%; AUC, 0.902; 95% CI, 0.834–0.970; $P < 0.001$). On the other hand, a score of VQAS >9.5 (sensitivity, 93.3%; specificity, 86.5%; AUC, 0.916; 95% CI, 0.843–0.988; $P < 0.001$) and SQNLP <81.1% (sensitivity, 86.5%; specificity, 86.7%; AUC, 0.944; 95% CI, 0.895–0.994; $P < 0.001$) was predictive of ICU admission (Fig. 7).

Both consolidation and CPP were more commonly seen in patients with severe pneumonia than patients with nonsevere pneumonia ($P = 0.197$ for consolidation; $P < 0.001$ for CPP) (Table 1). While presence of CPP showed severe pneumonia with 47.4% sensitivity, 97.2% specificity, 87.3% negative predictive value (NPV) and 81.8%

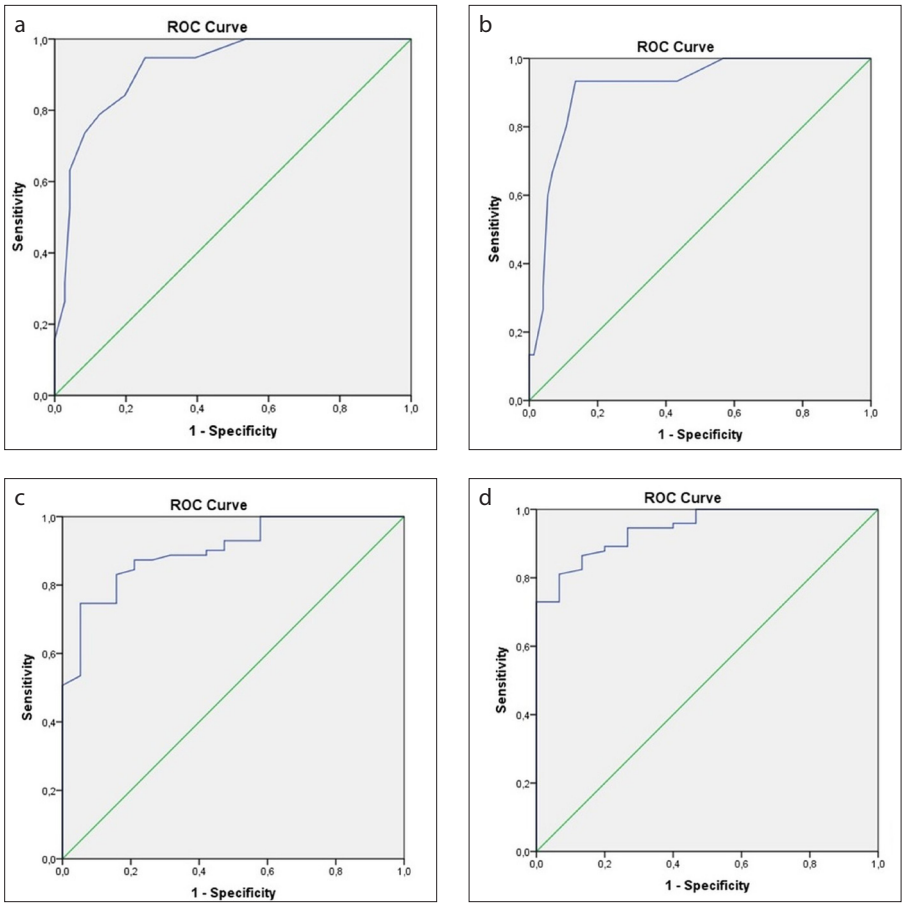

Figure 7. a–d. Receiver-operating characteristics (ROC) curves illustrate the ability of VQAS and SQNLP for predicting severe pneumonia and ICU admission. The area under the ROC curves (AUCs) are: **(a)**, 0.916 for VQAS and severe pneumonia; **(b)**, 0.916 for VQAS and ICU admission; **(c)**, 0.902 for SQNLP and severe pneumonia; 0.944 for SQNLP and ICU admission.

positive predictive value (PPV), presence of consolidation indicated severe pneumonia with 63.2% sensitivity, 53.5% specificity, 84.4% NPV and 26.7% PPV.

Discussion

The major finding of the current study was that both SQNLP and VQAS were significantly related to the clinical findings such as severe pneumonia, admission to ICU and length of hospital stay. While VQAS >8.5 and SQNLP <82.45% can show severe pneumonia, VQAS >9.5 and SQNLP <81.1% can predict ICU admission with high sensitivity and specificity.

Quantitative CT analysis with software has been used for evaluation and management of diffuse lung diseases including obstructive, infiltrative and restrictive pathologies. SQNLP can give valuable and objective information about COVID-19 pneumonia due to the infiltrative nature of lung involvement as part of the disease. Huang et al. (10) have recently found significant differences in the percentage of lung opacification, as measured by deep learning algorithm, among COVID-19 patients with different clinical severities. In SQNLP, attenuation values between -300 and -750 HU usually show GGO, while attenuation values lower than -950 HU demonstrate areas with emphysema (11, 15). Thus, attenuation values between -750 and -950 can show normal aerated lung parenchyma in COVID-19 pneumonia. Calculating normal lung parenchyma percentage avoids both the inadequate extraction of vessels which have similar density with lung opacities and the possible harmful effects of underlying lung abnormalities such as emphysema or lung fibrosis in patients with COVID-19. Chronic lung disease is one of the main risk factors for poor outcome and radiologic findings in the unaffected lung parenchyma is also important for the management and prognostication of patients (16). A recent study has found that a value of less than 71% of well-aerated lung tissue according to software-based assessment could predict ICU admission or death in patients with COVID-19 (9). In the current study, SQNLP <81.1% can predict ICU admission with 86.5% sensitivity and 86.7% specificity. The reason for our higher cutoff value may be because of earlier diagnosis and less ICU admissions in our cohort. Also, there was only a single mortality among our patients. Furthermore, SQNLP <82.45% can show severe pneumonia with 83.1% sensitivity and 84.2% specificity according to our results. SQNLP was found to be negatively correlated with old age, respiratory rate, high fever, troponin, D-dimer, ferritin, LDH, CRP, fibrinogen, procalcitonin, and positively correlated with sodium and albumin. These laboratory findings are also the ones that differ the most between patients with severe pneumonia and patients with non-severe pneumonia. Furthermore, lower SQNLP was related to male gender and dyspnea.

Although the number of males and females was similar in this cohort, COVID-19 pneumonia was more severe in men than women similar to the findings in recent studies (17, 18). Male gender showed significantly higher values of VQAS, and lower values of SQNLP. Similarly, older age was found significantly related to severe pneumonia, CPP, higher values of VQAS, and lower values of SQNLP like in recent studies (18, 19).

The most common presenting symptoms were dry cough, fever, and weakness in our study. But only dyspnea was significantly more common in patients with severe pneumonia and was significantly related with higher values of VQAS, CPP and lower values of SQNLP. Similar to our findings, Chen et al. (20) have observed fever, cough and fatigue as the most common manifestations and found dyspnea more frequently in severe cases, compared with moderate cases. The probable cause of this finding is that dyspnea primarily indicates lung involvement. On the other hand, anosmia showed lower values of VQAS and CPP, and higher values of SQNLP. Most of the patients with COVID-19 can have anosmia without nasal obstruction or rhinorrhea. Moreover, anosmia was defined more frequently in younger female patients with fewer comorbidities (21, 22). Thus, anosmia can be related to mild disease according to our results and recent studies.

All of the clinical and laboratory findings showing significant relationship with SQNLP were also found to be correlated with VQAS. Moreover, a cutoff value of VQAS

Table 3. Statistically significant clinical and laboratory findings according to the radiological scores

	VQAS	SQNLP	Consolidation	CPP
Age	r= 0.379	rs= -0.281	*P* = 0.778	*P* = 0.003
	P < 0.001	*P* = 0.007		
Sex (F/M)	*P* = 0.004	P = 0.022	*P* = 0.833	*P* = 0.052
Comorbidity	*P* = 0.012	P = 0.084	*P* = 0.655	*P* = 0.038
High fever at admission	r= 0.348	rs= -0.360	*P* = 0.582	*P* = 0.041
	P = 0.001	*P* = 0.001		
Anosmia	*P* < 0.001	*P* = 0.006	*P* = 0.612	*P* = 0.03
Dyspnea	*P* = 0.001	*P* = 0.011	*P* = 0.178	*P* = 0.001
Troponin	rs= 0.344	rs= -0.226	*P* = 0.811	*P* = 0.076
	P = 0.007	*P* = 0.013		
Ferritin	rs= 0.503	rs= -0.478	*P* = 0.372	*P* = 0.002
	P < 0.001	*P* = 0.001		
LDH	rs= 0.566	rs= -0.551	*P* = 0.004	*P* = 0.043
	P < 0.001	*P* < 0.001		
CRP	rs= 0.647	rs= -0.603	*P* = 0.074	*P* = 0.003
	P < 0.001	*P* < 0.001		
Fibrinogen	r= 0.420	rs= -0.366	*P* = 0.138	*P* = 0.011
	P < 0.001	*P* = 0.001		
D-dimer	rs= 0.428	rs= -0.397	*P* = 0.010	*P* = 0.005
	P < 0.001	*P* = 0.001		
Sodium	rs= -0.326	rs= 0.264	*P* = 0.187	*P* = 0.026
	P = 0.002	*P* = 0.012		
Albumin	rs= -0.375	rs= 0.365	*P* = 0.061	*P* = 0.051
	P = 0.001	*P* = 0.001		
Procalcitonin	rs= 0.427	rs= -0.372	*P* = 0.367	*P* = 0.031
	P < 0.001	*P* < 0.001		
Respiratory rate	rs= 0.511	rs= -0.496	*P* = 0.079	*P* = 0.027
	P < 0.001	*P* = 0.001		
Length of hospital stay	rs= 0.516	rs= -0.434	*P* = 0.974	*P* = <0.001
	P < 0.001	*P* < 0.001		
Admission to ICU	*P* < 0.001	*P* < 0.001	*P* = 0.087	*P* = 0.001
Presence of severe pneumonia	*P* < 0.001	*P* < 0.001	*P* = 0.197	*P* < 0.001

VQAS, visual quantitative assessment score; SQNLP, software-based quantitative assessment of the normal lung parenchyma percentage; CPP, crazy paving pattern; F/M, female/male; LDH, lactate dehydrogenase; CRP, C-reactive protein; ICU, intensive care unit.

>8.5 can show severe pneumonia and VQAS >9.5 can predict ICU admission with higher sensitivity and specificity. Using another CT scoring system that ranged from 0 to 40, Yang et al. (23) have defined a threshold of 19.5 for identifying severe pneumonia with 83.3% sensitivity and 94% specificity.

Besides predicting ICU admission and severe pneumonia, both VQAS and SQNLP show significant correlation with length of hospital stay according to our results. Similar to ours, another recent study has found independent association between extended hospitalization and CT-based lung severity score, which ranged from 0 to 20 (24). Thus, both VQAS and SQNLP can be used for predicting ICU admission and help the clinicians in the management of patients with COVID-19 pneumonia.

There are various studies about CT score systems that are based on visual assessment of the percentage of opacities (8, 13, 23, 25). Besides percentage of opacities, presence of consolidation and CPP can show difference in clinical findings (25, 26). Huang et al. (14) have defined another scoring system including consolidation and CPP. For demonstrating the effect of consolidation and CPP, we evaluated the presence of consolidation and CPP separately.

In our study, both CPP and consolidation were more common in patients with severe pneumonia, but the presence of CPP was found to have high specificity (97.2%) for severe pneumonia. CPP consists of GGO with superimposed interlobular septal thickening and intralobular lines. In patients with COVID-19, diffuse alveolar damage has been defined with interstitial edema, thickening of alveolar walls and proliferation of interstitial fibroblasts (27). CPP can be secondary to these pathologic findings. In addition, platelet-fibrin thrombi in small vessels, small vessels hyperplasia, and vessel wall thickening have been described in pathologic investigation of patients with COVID-19 (28, 29). A recent study has found that the pattern of COVID-19 pneumonitis was predominantly a pauci-inflammatory septal injury with significant septal capillary mural and luminal fibrin deposition (30). These vascular findings may be another reason for inter and intralobular lines of CPP in COVID-19 pneumonia, like pulmonary veno-occlusive disease, in which thickening of interlobular septa was observed due to microvascular occlusion and edema (31). Thus, the higher specificity of CPP for severe pneumonia in the current study may be secondary to these pathologic findings which might be the harbingers of severe disease.

Some limitations of our study merit consideration. The major limitation of the study was the relatively small sample size of the groups, particularly for severe pneumonia, ICU admission, and CPP. Another limitation was inappropriate segmentation of some images. Because of this reason, some patients were excluded from the study and lung contours were corrected by a radiologist for the others. Finally, as the images at the expiratory phase were not included in the study, in some images SQNLP could not calculate small areas at the threshold of -750 HU.

In conclusion, both SQNLP and VQAS were significantly related to the clinical findings, and both might be helpful in predicting severe pneumonia, ICU admission, and management of disease. Although both CPP and consolidation were more

commonly seen in patients with severe pneumonia, presence of CPP has high specificity for severe pneumonia. Future studies with larger sample sizes can provide better understanding of the effects of quantitative chest CT assessments and CPP in patients with COVID-19 pneumonia.

Conflict of interest disclosure

The authors declared no conflicts of interest.

References

1. Huang C, Wang Y, Li X, et al. Clinical features of patients infected with 2019 novel coronavirus in Wuhan, China. Lancet 2020; 395:497–506. [Crossref]
2. Lu R, Zhao X, Li J, et al. Genomic characterisation and epidemiology of 2019 novel coronavirus: implications for virus origins and receptor binding. Lancet 2020; 395:565–574. [Crossref]
3. Wang D, Hu B, Hu C, et al. Clinical characteristics of 138 hospitalized patients with 2019 novel coronavirus-infected pneumonia in Wuhan, China. JAMA 2020; 323:1061–1069. [Crossref]
4. Xu Z, Shi L, Wang Y, et al. Pathological findings of COVID-19 associated with acute respiratory distress syndrome. Lancet Respir Med 2020; 8:420–422. [Crossref]
5. Ai T, Yang Z, Hou H, et al. Correlation of chest CT and RT-PCR testing in coronavirus disease 2019 (COVID-19) in China: a report of 1014 cases. Radiology 2020 Feb 26. [Epub Ahead of Print] [Crossref]
6. Fang Y, Zhang H, Xie J, et al. Sensitivity of chest CT for COVID-19: comparison to RT-PCR. Radiology 2020 Feb 19. [Epub Ahead of Print] [Crossref]
7. Chung M, Bernheim A, Mei X, et al. CT imaging features of 2019 novel coronavirus (2019-nCoV). Radiology 2020; 295:202–207. [Crossref]
8. Li K, Fang Y, Li W, et al. CT image visual quantitative evaluation and clinical classification of coronavirus disease (COVID-19). Eur Radiol 2020 Mar 25. [Epub Ahead of Print] [Crossref]
9. Colombi D, Bodini FC, Petrini M, et al. Well-aerated lung on admitting chest CT to predict adverse outcome in COVID-19 pneumonia. Radiology 2020 Apr 17. [Epub Ahead of Print] [Crossref]
10. Huang L HR, Ai T, Yu P, Kang H, Tao Q, Xia L. Serial quantitative chest CT assessment of COVID-19: deep-learning approach. Radiology 2020 Mar 30. [Epub Ahead of Print] [Crossref]
11. Chen A, Karwoski RA, Gierada DS, Bartholmai BJ, Koo CW. Quantitative CT Analysis of Diffuse Lung Disease. Radiographics 2020; 40:28–43. [Crossref]
12. T.C. Sağlık Bakanlığı Halk Sağlığı Genel Müdürlüğü, COVID-19 (SARS-CoV-2 Enfeksiyonu) Rehberi, Erişkin Hasta Tedavisi, Bilimsel Danışma Kurulu Çalışması, 2020.
13. Pan F, Ye T, Sun P, et al. Time course of lung changes on chest ct during recovery from 2019 novel coronavirus (COVID-19) pneumonia. Radiology 2020 Feb 13. [Epub Ahead of Print] [Crossref]
14. Huang G, Gong T, Wang G, et al. Timely diagnosis and treatment shortens the time to resolution of coronavirus disease (COVID-19) pneumonia and lowers the highest and last CT scores from sequential chest CT. AJR Am J Roentgenol 2020:1–7. [Crossref]
15. Kauczor HU, Heitmann K, Heussel CP, Marwede D, Uthmann T, Thelen M. Automatic detection and quantification of ground-glass opacities on high-resolution CT using multiple neural networks: comparison with a density mask. AJR Am J Roentgenol 2000; 175:1329–1334. [Crossref]
16. Akpinar E, Erbil B. Is CO-RADS a categorical chest CT assessment scheme or a suspicion scale only? Radiology 2020 May 13. Available from: https://pubs.rsna.org/page/radiology/blog/2020/5/brief_communications_202094
17. Li X, Xu S, Yu M, et al. Risk factors for severity and mortality in adult COVID-19 inpatients in Wuhan. J Allergy Clin Immunol 2020 Apr 12. [Epub Ahead of Print] [Crossref]
18. Shi Y, Yu X, Zhao H, Wang H, Zhao R, Sheng J. Host susceptibility to severe COVID-19 and establishment of a host risk score: findings of 487 cases outside Wuhan. Crit Care 2020; 24:108. [Crossref]
19. Borghesi A, Zigliani A, Masciullo R, et al. Radiographic severity index in COVID-19 pneumonia: relationship to age and sex in 783 Italian patients. Radiol Med 2020; 125:461–464. [Crossref]
20. Chen G, Wu D, Guo W, et al. Clinical and immunological features of severe and moderate coronavirus disease 2019. J Clin Invest 2020; 130:2620–2629. [Crossref]
21. Klopfenstein T, Kadiane-Oussou NJ, Toko L, et al. Features of anosmia in COVID-19. Med Mal Infect 2020 Apr 17. [Epub Ahead of Print] [Crossref]
22. Lechien JR, Chiesa-Estomba CM, De Siati DR, et al. Olfactory and gustatory dysfunctions as a clinical presentation of mild-to-moderate forms of the coronavirus disease (COVID-19): a multicenter European study. Eur Arch Otorhinolaryngol 2020 Apr 6. [Epub Ahead of Print]
23. Yang R LX, Liu H, Zhen Y, et al. Chest CT Severity Score: An Imaging Tool for Assessing Severe COVID-19. Radiology 2020 Mar 30. [Epub Ahead of Print] [Crossref]
24. Liu Z, Jin C, Wu CC, et al. Association between-sinitial chest ct or clinical features and clinical course in patients with coronavirus disease 2019 pneumonia. Korean J Radiol 2020; 21:736–745. [Crossref]
25. Lyu P, Liu X, Zhang R, Shi L, Gao J. The performance of chest CT in evaluating the clinical severity of COVID-19 pneumonia: identifying critical cases based on CT characteristics. Invest Radiol 2020 Apr 16. [Epub Ahead of Print] [Crossref]
26. Li K, Wu J, Wu F, et al. The clinical and chest CT features associated with severe and critical COVID-19 pneumonia. Invest Radiol 2020; 55:327–331. [Crossref]
27. Tian S, Hu W, Niu L, Liu H, Xu H, Xiao SY. Pulmonary pathology of early-phase 2019 novel coronavirus (COVID-19) pneumonia in two patients with lung cancer. J Thorac Oncol 2020; 15:700–704. [Crossref]
28. Luo W, Yu H, Gou J, et al. Clinical pathology of critical patient with novel coronavirus pneumonia (COVID-19). Preprints 2020; 2020020407.
29. Carsana L, Sonzogni A, Nasr A, et al. Pulmonary post-mortem findings in a large series of COVID-19 cases from Northern Italy. medRxiv. 2020:2020.04.19.20054262. [Crossref]
30. Magro C, Mulvey JJ, Berlin D, et al. Complement associated microvascular injury and thrombosis in the pathogenesis of severe COVID-19 infection: a report of five cases. Transl Res 2020 Apr 15. [Epub Ahead of Print] [Crossref]
31. Frazier AA, Franks TJ, Mohammed TL, Ozbudak IH, Galvin JR. From the Archives of the AFIP: pulmonary veno-occlusive disease and pulmonary capillary hemangiomatosis. Radiographics 2007; 27:867–882. [Crossref]